Section-specific H^+ fluxes in renal tubules of fasted and fed goldfish

Sandra Fehsenfeld[1,2$], Dennis Kolosov[3], Chris M. Wood[1,3], Michael J. O'Donnell[3]

[1]University of British Columbia, Department of Zoology, Vancouver, Canada

[2]Université du Québec à Rimouski, Département de Biologie, Chimie et Géographie, Rimouski, Canada

[3]McMaster University, Department of Biology, Hamilton, Canada

Orcid IDs: SF:0000-0003-4495-8715; DK: 0000-0003-3581-9991; MJO: 0000-0003-3988-6059;

CMW: 0000-0002-9542-2219

[$]Corresponding author

Email address: Sandra.Fehsenfeld@uqar.ca

Phone: +1 (204) 296-2106

Université du Québec à Rimouski

Département de Biologie, Chimie et Géographie

300 Allée du Ursulines

Rimouski, QC

Canada - G5L 3A1

Keywords: freshwater teleost, renal epithelium, acidosis, SIET

Abstract

A recent study demonstrated that in response to a feeding-induced metabolic acidosis, goldfish *Carassius auratus* adjust epithelial protein and/or mRNA expression in their kidney tubules for multiple transporters known to be relevant for acid-base regulation. These include Na^+/H^+-exchanger, V-H^+-ATPase, cytoplasmic carbonic anhydrase, HCO_3^--transporters, and Rhesus proteins. Consequently, renal acid output in the form of protons and NH_4^+ increases. Little, however, is known about mechanistic details of renal acid-base regulation in *C. auratus* and teleost fishes in general. The present study applied the Scanning Ion-selective Electrode Technique (SIET) to measure proton flux in proximal, distal and connecting tubules of goldfish. We detected increased H^+ efflux into the extracellular fluid from the tubule in fed animals, resulting from paracellular back-flux of H^+ through the tight junction. By applying inhibitors for selected acid-base regulatory epithelial transporters, we found that cytosolic carbonic anhydrase and HCO_3^- transporters were important in mediating H^+ flux in all three tubule segments of fed goldfish. Contrastingly, V-H^+-ATPase seemed to play a role for H^+ flux only in proximal and distal tubule, and Na^+/H^+-exchanger in proximal and connecting tubule. We develop working models for transport of acid-base relevant equivalents (H^+, HCO_3^-, NH_3/NH_4^+) for each tubule segment in *C. auratus* kidney. While the proximal tubule appears to play a major role in both H^+ secretion and HCO_3^- reabsorption, the distal and connecting tubules seem to mainly serve for HCO_3^- reabsorption and NH_3/NH_4^+ secretion.

Introduction

The maintenance of acid-base homeostasis is one of the most important physiological processes in all organisms as it ensures proper enzyme and protein function (Somero, 1986; Riggs, 1988). The kidney has the predominant function of generating and transporting HCO_3^- and ammonia (here referred to as the sum of NH_3 and NH_4^+) in mammals, and thus ultimately regulates any metabolic acid-base disturbances by adjusting net acid (both titratable acid and NH_4^+ fluxes) and base (HCO_3^-) excretion (Hamm et al., 2015). In teleost fishes, by contrast, the predominant organ involved in regulating acid-base disturbances is the gill (Perry and Gilmour, 2006), while the kidney seems to play only a small but significant role in acid-base balance. For instance, the kidney of the freshwater rainbow trout, *Oncorhynchus mykiss*, is known to compensate for environmental disturbances that induce acidosis, such as exposure to low environmental pH (McDonald and Wood, 1981), hyperoxia (Wheatly et al., 1984), hypercapnia (Perry and Fryer, 1997), and exhaustive exercise (Wood, 1988), as well as for a feeding-induced alkaline tide (Bucking et al., 2010). The mechanisms of renal ammonia and acid-base regulation in teleosts, however, remain poorly studied to date. This difficulty stems, in part, from the structural heterogeneity and architectural complexity of the teleost kidney, which contains multiple tissue types and a convoluted tubule (Sakai, 1985). Consequently, most physiological studies have only investigated acid-base regulation by the kidney as a whole (e.g. Wood et al. 1999; Lawrence et al. 2015; Wright et al. 2014). However, recently, Fehsenfeld and Wood (2018) micro-dissected the kidney of the goldfish, *Carassius auratus*, enabling them to profile mRNA and protein expression of renal epithelial transporters involved in acid-base homeostasis along the renal tubule and its different segments.

In general, renal ionoregulation in freshwater teleosts involves epithelial transporters that are important for the re-absorption of ions to minimize solute loss into the dilute external medium (Wheatly et al., 1984; Curtis and Wood, 1992; Perry et al., 2003b). Transport of primary ions and electrolytes is coupled to the transport of acid-base equivalents, hence linking ionoregulation and acid-base balance in the teleost kidney (Perry et al. 2003b; Wheatly et al. 1984; Dantzler 2016). Many of the same transporters, including V-H^+-ATPase, Na^+/H^+-exchanger, Na^+/HCO_3^--cotransporter and HCO_3^-/Cl^--exchanger, can also be found in the teleost gill epithelium (Perry et al., 2003b). Similarly, these transporters are involved in acid-base regulation in the mammalian kidney (Weiner and Verlander, 2013).

In fasting *C. auratus*, the kidney produces alkaline urine, resulting in net renal base excretion. Exposure of animals to a low pH environment, however, results in net renal acid excretion (Lawrence et al. 2015). In contrast to the rainbow trout, the goldfish is agastric like the freshwater killifish *Fundulus heteroclitus* (Wood et al., 2010), having an alkaline digestive tract and therefore exhibits a systemic acidic tide after feeding. Fehsenfeld and Wood (2018) were able to show that a systemic acid-load (metabolic acidosis) caused by feeding resulted in increased acid excretion by the goldfish kidney as indicated by a decrease in urine pH and increase in urine inorganic phosphate and ammonia concentrations. This process was in part accomplished by differentially adjusting expression levels of both mRNA and protein of a variety of transporters in the proximal, distal and connecting tubule of the goldfish nephron (Fehsenfeld and Wood, 2018).

The present study aimed to further investigate the mechanism of renal acid-base regulation in response to feeding in *C. auratus*. Micro-dissection of intact kidney tubules in combination with the Scanning Ion-selective Electrode Technique (SIET) (Smith et al., 1994;

Pineros et al., 1998) allowed for the direct measurement of H^+ flux at the basolateral surface of distinct segments of the renal tubule. Measurements from fasted and fed goldfish were used to demonstrate the effects of feeding on the acid-base transport physiology of the proximal, distal and connecting tubule. Furthermore, with the application of specific inhibitors, we were able to identify epithelial transporters involved in renal acid-base regulation by promoting and/or inhibiting H^+ fluxes in the various renal tubule segments. We hypothesized that V-H^+-ATPase, Na^+/H^+-exchanger, HCO_3^--transporters (Na^+/HCO_3^--cotransporter and/or HCO_3^-/Cl^--exchanger) and carbonic anhydrase (the enzyme converting CO_2 to H^+ and HCO_3^- and vice versa) contribute to the H^+ flux through the renal epithelium. Furthermore, we hypothesized that (i) H^+ fluxes would differ among the segments of the renal tubule and (ii) would be differentially affected by the inhibitors, due to differential expression of the transporters (mRNA and protein level) in each tubule segment as shown by Fehsenfeld and Wood (2018).

Materials and methods

Animal care

Goldfish (~5 cm / 2.5-3.0 g) were obtained from commercial suppliers and were held in 20-L aquaria at room temperature at a maximum density of 1 fish / 2-L for a minimum of 7 days before being sacrificed for the experiments. The recirculating and filtered tap water composition was (in mequiv/l): 0.6 Na^+, 0.8 Cl^-, 1.8 Ca^{2+}, 0.3 Mg^{2+}, 0.05 K^+; titration alkalinity 2.1; hardness ~140 mg/l as $CaCO_3$ equivalents. Water parameters (pH = 7.4, ammonia, nitrate and nitrite) were closely monitored and water changes performed 2-3 times a week as necessary. Fish were fed to satiation 2-3 times a week with commercial flaked food (Nutrafin Max, Hagen, Montreal, Canada). For experiments, fish were either fasted for 96 h and then sacrificed (“fasted”), or

fasted for 93h, then fed to satiation, and sacrificed 3 h after feeding ("fed"). Each animal was sacrificed by cephalic concussion. All procedures were conducted under the approval of the University of British Columbia Animal Care Committee (licence no. A14-0251) and the guidelines of the Canadian Council on Animal Care.

Preparation of renal tubules for measurements

Immediately after sacrifice, the kidney was removed and transferred into control goldfish Ringer containing (in mmol L^{-1}): 100.0 NaCl, 2.5 KCl, 1.5 $CaCl_2 \bullet 2H_2O$, 1.0 $MgCl_2 \bullet 6H_2O$, 5.0 $NaHCO_3$, 0.7 $NaH_2PO_4 \bullet H_2O$, 10 glucose, pH = 7.3 (modified after Hoar and Hickman 1975). First, larger clusters of tubules were pulled from the Wolffian duct as it runs through each half of the kidney. Subsequently, minuten pins glued to needles and screwed into syringes for better handling were used to carefully isolate single tubules including the glomerulus, proximal tubule, distal tubule and connecting tubule out of these clusters, as described in Fehsenfeld and Wood (2018). One intact tubule was transferred into the lid of a 5 cm Nunc cell culture dish and pinched down onto the dish at both ends using the needles. Lids, rather than the bottom part of the dishes, were used because tubules would stick to them due to apparent adhesive forces holding them in place that did not seem to be present in the bottom dish. The preparation was then transferred into the Scanning Ion-selective Electrode Technique (SIET) set-up and measurements were started immediately in control goldfish Ringer.

Measurement of renal H^+ fluxes by SIET

SIET hardware was obtained from Applicable Electronics (New Haven, CT, USA) and Automated Scanning Electrode Technique version 2 (ASET2) software from Science Wares (Falmouth, MA, USA). Hardware, software and methodology for acquiring SIET data and calculating ion fluxes have been described in detail in previous publications (Donini and O'Donnell, 2005; Pacey and O'Donnell, 2014; D'Silva et al., 2017). Briefly, ion-selective microelectrodes were pulled to a ~5 µm tip diameter using a programmable P-97 micropipette puller (Sutter Instruments, Novato, CA, USA). Silanized microelectrodes were back-filled with 100 mM NaCl/100 mM sodium citrate (pH 6.0). Electrodes were then tip-filled with ~200 µm column length of H^+ Ionophore I Cocktail B (Millipore Sigma, Burlington, MA, USA). Slopes of microelectrodes calibrated in pH=6.5 and pH=7.5 solutions were 59.5 ± 0.4 mV per ten-fold change in H^+ concentration. Voltage gradients obtained using SIET readings were converted into concentration gradients and subsequently into flux using Fick's law applying the following equations from Donini and O'Donnell (2005):

Concentration gradient: $$\Delta C = C_B \times 10^{\Delta V/S} - C_B$$

Fick's law: $$J_I = D_I(\Delta C)/\Delta x$$

where ΔC is the concentration gradient in mol cm^{-3}; C_B is the background ion concentration, (calculated as the average of the concentration at each point) in µmol L^{-1}; ΔV is the voltage gradient obtained from the software ASET2 in µV; S is the slope of the electrode; J is the flux in mol cm^{-2} s^{-1}, D is the diffusion coefficient in cm^2 s^{-1}, and Δx is the distance between the two points in cm. Buffering capacity (x_i) for H_2O, HCO_3^-, and $H_2PO_4^-$, their diffusion coefficients (D_B) (H_2O, D_B = 9.31 E-05 / HCO_3^-, D_B = 1.20 E-05 / $H_2PO_4^-$, D_B = 8.30 E-06)) and acid

dissociation constants (Ka) were taken into account to adjust H^+ flux values for the buffering capacity of the measuring media as follows (Messerli et al., 2006):

Buffering capacity: $x_i = Ka/(Ka+[H^+])^2 * D_B/D_{H+} * [buffer]$

Corrected H^+ flux: $J_{H+total} = J_{H+\ measured}\,(1 + x_{HCO3-} + x_{H2PO4-} + x_{H2O})$

To determine control H^+ fluxes in fasted and fed animals, renal tubules were scanned in control goldfish Ringer in 100 μm increments starting at the glomerulus and ending at the connecting tubule. To test for potential effects of time on tissue viability, the goldfish Ringer was renewed after the first scan, the tubules incubated for 10 min (to mimic addition of inhibitors as described below), and then rescanned at the same positions. For the investigation of the effects of inhibitors on proton fluxes, the tubules of fed goldfish were incubated with the respective inhibitor for 10 min after the control scan, and then rescanned at the same locations as for the control Ringer. Inhibitors and their concentrations (and targets) were: 10 mmol L^{-1} 2,4,6-triaminopyrimidine (TAP; paracellular pathway), 100 μmol L^{-1} 5-(N-ethyl-N-isopropyl)amiloride (EIPA; Na^+/H^+-exchanger), 100 μmol L^{-1} 4,4'-diisothiocyanatostilbene-2,2'-disulfonate (DIDS; HCO_3^-/Cl^--exchanger and/or Na^+/HCO_3^--cotransporter), 5 μmol L^{-1} bafilomycin (V-H^+-ATPase), and 1μmol L^{-1} acetazolamide (carbonic anhydrase). There was no effect of the inhibitors at the indicated concentrations on the slope/responsiveness of the H^+ microelectrodes.

Statistical analysis

Data are expressed as means ± SE (N), where N represents the number of animals. All statistical analyses were performed with PAST3 (Hammer et al., 2001) or Minitab® Statistical Software (State College, PA, USA). Data were checked for normal distribution with the Shapiro-Wilks test

and homogeneity of variances with the F-test. If data did not meet these criteria for parametric testing, they were log-transformed.

To investigate the effect of feeding (Fig. 1) and/or time (Fig. 2) on tubular H^+ flux, the mean H^+ flux for each segment (proximal, distal and connecting tubule) was calculated for fasted and fed animals (indicated by horizontal lines; Fig. 1, 2), respectively. Data were then analyzed by two-way ANOVA using a general linear model as implemented in Minitab 18 (Fig. 1: factor 1 = fasted vs. fed, factor 2 = tubule segment; Fig. 2: repeated measures two-way ANOVA, factor 1 = 1^{st} run vs. 2^{nd} run, factor 2 = tubule segment). Subsequently, pairwise comparisons were conducted using Tukey's post-hoc test.

For the inhibitor experiments (Figures 4-6), Student's paired t-tests were applied for each inhibitor in each section. Data were considered significantly different at $P \leq 0.05$. All graphs were generated with Inscape 0.92.0 r15299 (https://www.inkscape.org).

Results

In fasted goldfish, H^+ efflux was observed from the tubule lumen and/or the epithelial cells over the basolateral epithelium to the external solution (Fig. 1B). Mean H^+ flux rates did not differ significantly between the different segments of fasted animals (Fig. 1A). Two-way ANOVA revealed a significant effect of both tubule segment and feeding status on H^+ flux, but not their interaction. Tukey's post hoc analysis identified H^+ flux in the distal tubule of fed animals to be significantly lower (-57%) compared to proximal and connecting tubule of fed animals. Mean proton fluxes increased significantly in fed animals compared to fasted animals in all three tubule segments (Tukey's post-hoc analysis), and were most pronounced in the proximal tubule (3.5-fold vs. 2.4 and 2.2-fold increases in distal and connecting tubule, respectively) (Fig. 1A, B).

H^+ fluxes during two consecutive runs with control saline in tubules of fed animals did not decrease significantly over time (Fig. 2; repeated measures two-way ANOVA). There was, however, a significant effect of tubule segment according to findings in fed tubules as mentioned above, with the distal tubule having significantly lower H^+ flux compared to both the proximal and connecting tubule (Tukey's post-hoc analysis). There was no significant interaction of time and tubule segment ($P = 0.7$).

Consequently, tubules from fed animals were used in testing the effects of inhibitors. The application of 2,4,6-triaminopyrimidine (TAP; 10 mmol L^{-1}) (Fig. 3) to inhibit the paracellular pathway resulted in a dramatic ~ 90% decrease of H^+ flux in all three segments. Targeting epithelial transporters and enzymes with specific inhibitors differentially affected H^+ fluxes along the tubule. Fig. 4 shows results in the proximal, Fig. 5 in the distal, and Fig. 6 in the connecting tubule. Inhibiting Na^+/H^+-exchanger with EIPA decreased H^+ flux by ~55% in the proximal and connecting tubule, but did not affect the distal tubule. Applying DIDS against HCO_3^--transporters resulted in a decrease of H^+ flux by 70% in the proximal tubule, and approximately 50% in the distal and connecting tubule. When V-H^+-ATPase was blocked by bafilomycin, H^+ flux decreased by 67% in the proximal and 45% in the distal tubule, while no effect was observed in the connecting tubule. Targeting carbonic anhydrase with acetazolamide decreased H^+ flux by roughly 60% in all three segments.

Discussion

General observations

Goldfish *Carassius auratus* produce an alkaline urine (pH 7.8 – 8.5) under fasted conditions (Lawrence et al., 2015; Fehsenfeld and Wood, 2018). This indicates renal reabsorption of H^+ from the tubule lumen into the extracellular fluid/plasma, and indeed, this is what we measured in the present study by applying the Scanning Ion-selective Electrode Technique (SIET) to the proximal, distal and connecting tubule (Fig. 1). In response to the acidic tide caused by feeding, however, urine pH was observed to drop by up to 0.6 units (Fehsenfeld and Wood 2018); under these conditions the kidney reverses this flux to net H^+-secretion. Surprisingly, the results here appear to show the opposite, suggesting a pronounced increase in H^+ reabsorption in response to feeding that was highest in the proximal tubule (3.5-fold vs. ~2.3-fold in distal and connecting tubule in reference to fasted conditions; Fig. 1). When the paracellular pathway was blocked with TAP, however, the observed H^+ reabsorption was reduced to 10% of the control values for fed animals in all segments (Fig. 3). The teleost kidney has been reported to express a multitude of tight junction proteins: cytosolic scaffolding proteins cingulin and ZO-1 (Kolosov et al., 2014), as well as transmembrane proteins like occludin (Chasiotis and Kelly, 2008; Kolosov et al., 2017) and over 35 claudins (Kolosov et al., 2013), and the tricellular proteins ILDR2 and tricellulin (Kolosov and Kelly, 2013, 2018; Kolosov et al., 2017). Despite the fact that many tight junction proteins have been detected in the kidney, their individual role and distribution in the different regions of the fish nephron are unknown. Chasiotis and Kelly, however, showed that occludin was expressed in the distal and not the proximal tubule of goldfish (Chasiotis and Kelly, 2008) and the African clawed frog *Xenopus laevis* (Chasiotis and Kelly, 2009).

Accordingly, rather than indicating a direct reabsorption of protons, the observed H^+ flux likely represents H^+ back-flux via the paracellular pathway down the concentration gradient established by active H^+-secretion into the small closed tubular lumen.

We are confident that the tissue was intact and that this H^+ back-flux was not due to tissue deterioration, because we took particular care to avoid touching the tubules themselves during the microdissection (i.e. they were not pulled on or squeezed). Rather, needles were mainly used to carefully tease apart the connective tissue. Additionally, we carefully inspected every tubule visually during and after the microdissection for any potential rips. Measurements were highly reproducible, and tubules of fasted animals generally had very low H^+-flux.

Since it was not possible to directly measure apical H^+ flux, the observed H^+ back-flux through the tight junction can be interpreted as a proxy for apical H^+ secretion. Consequently, a proton gradient directed from the lumen to the plasma, resulting in the observed H^+ back-flux, can be explained by the following: (1) active apical ion transport resulting in higher $[H^+]$ in the tubular lumen compared to extracellular $[H^+]$, and/or (2) "trapped" urine of fed animals having already increased $[H^+]$ in the lumen (pH = 7.2) compared to the extracellular fluid (pH = 7.85 of fasted animals (Fehsenfeld and Wood, 2018)). Differences in the magnitude of H^+ back-flux in the different segments of the tubule isolated from fed animals (Fig. 1A) can be attributed to a combination of regional alterations in (i) paracellular permeability, i.e. the tight junctions, and (ii) active ion transporter (epithelial channels and pumps) expression. In the intact kidney of fed freshwater fishes, such back-flux of H^+ through the paracellular cleft would be minimized by continuous production and flow of copious amounts of dilute urine that would likely increase in the face of a systemic acidosis (Lawrence et al., 2015).

Effects of ion transporter inhibitors targeting epithelial transporters on proton flux

While the recent study by Fehsenfeld and Wood (2018) established a general molecular basis for renal acid-base regulation in different tubule segments of the goldfish kidney, the SIET measurements of the present study allowed us to establish real-time H^+ flux data. Furthermore, by application of specific inhibitors, our results here allow us to compare the observed H^+ flux to the presence of epithelial transport proteins and further characterize their role in renal acid-base balance in the different tubule segments. Note that we elected to test the potential inhibitors only on preparations from fed animals, because H^+ flux rates were low in fasted animals, so we cannot eliminate the possibility that different response patterns would have been seen in the latter.

Here, we suggest models for general mechanisms of transport of acid-base equivalents (i.e. H^+, HCO_3^- and NH_4^+) in the proximal (Fig. 7), distal (Fig. 8), and connecting tubule (Fig. 9). No inhibitors are currently available for Rhesus proteins, the major transporters for NH_3/NH_4^+. They are, however, likely to play a role in acid-base regulation, so we have incorporated them into our proposed models where appropriate. The models take into account inhibitor results from the present study, protein and mRNA expression data from Fehsenfeld and Wood (2018), as well as aspects from the mammalian models for renal acid-base (Hamm et al. 2013) and ammonia transport (Weiner and Verlander, 2013, 2017). While depicted here as one cell, it is possible that certain processes are rather associated with multiple rather specific cell types as in the mammalian system.

Na^+/H^+-exchanger

Na^+/H^+ -exchanger (NHE) is generally believed to promote apical H^+-secretion (and Na^+-absorption) in the vertebrate kidney and specifically in the proximal tubule as the major site for renal acid excretion (Gilmour and Perry, 2009; Hamm et al., 2013). Furthermore, protein abundance of NHE (isoform 3) in the cortical brush-border apical membrane of the proximal tubule was reported to increase following chronic metabolic acidosis in rats (Ambühl et al., 1996). Likewise, in goldfish renal tubules, NHE3 protein was located in the basolateral membrane of all tubule segments of fasted goldfish, but increased in abundance and relocated to the apical membrane in the proximal tubule when animals experienced a systemic acid-load due to feeding (Fehsenfeld and Wood, 2018). This indicates a similar mechanism in the goldfish kidney to that in the mammalian kidney.

Blockade of NHE(s) with the pharmaceutical EIPA in the present study resulted in a decrease of H^+ flux in the goldfish renal tubule verifying its role in renal acid-base balance. Surprisingly, however, this was only observed in the proximal (Fig. 4) and the connecting tubule (Fig. 6) of fed goldfish, and not in the distal segment (Fig. 5). It has to be kept in mind that the inhibitor may have acted not only on basolateral but also apical NHE3 due to its permeability through the tight junctions (Van Itallie et al., 2008; Hou et al., 2013). Consequently, the decrease of H^+ flux in the proximal tubule when inhibited by EIPA is in line with NHE-mediated apical proton secretion. Alternately or additionally, EIPA may have blocked a different isoform of NHE, for example NHE1 that appears to be expressed in the basolateral membrane of the proximal tubules in mammals (Hamm et al. 2013; Bobulescu et al. 2005). NHE may be present

in the distal segment of goldfish, but in accordance to our measurements is likely not involved in acid-base regulation in this region as has been suggested also for the mammalian distal tubule (Hamm et al. 2013).

HCO_3^- transporters

An electrogenic Na^+/HCO_3^- -cotransporter (NBCe1A/NBC1) in basolateral membranes of the proximal tubule is crucial for the reabsorption of base in mammals (Hamm et al., 2013; Weiner and Verlander, 2013; Handlogten et al., 2015). NBC1 has also been identified in the trout kidney and was proposed to mediate increased basolateral reabsorption of HCO_3^- in response to a respiratory acidosis caused by hypercarbia (Perry et al. 2003a). Two anion exchangers have been identified in mammalian renal cells: AE1 (SLC4A1) is present in in the basolateral membrane of A-type intercalated cells (A-ICs) in the collecting duct, whereas pendrin (SLC26A4) is found in the apical membrane of the proximal tubule and A-type intercalated cells (B-ICs) of the collecting duct (Hamm et al. 2013; Soleimani et al. 2001). Members of the SLC26-family of membrane transporters including pendrin have also been identified in zebrafish gills (Bayaa et al., 2009) and in V-H^+-ATPase-rich cells in the elasmobranch branchial epithelium (Piermarini and Evans, 2001; Tresguerres et al., 2005; Reilly et al., 2011). In response to a metabolic alkalosis (feeding-induced alkaline tide), elasmobranch gills translocated pendrin into the apical membrane with the help of cytoplasmic carbonic anhydrase (Tresguerres et al., 2007; Roa et al., 2014). NBC1 and AE1 on the other hand were expressed basolaterally not only in the proximal, but also the distal and connecting tubule in goldfish (Fehsenfeld and Wood, 2018).

Unfortunately, no specific inhibitor can distinguish between NBC(s), AE(s) and/or pendrin (Soleimani et al., 2001; Bayaa et al., 2009). The application of DIDS, as chosen here to

block HCO_3^- -transporters in general, resulted in a decrease of proton flux in all three segments but was most pronounced in the proximal segment (70% inhibition of H^+ flux, vs. 50% in distal and connecting tubule; Figs 4, 5, 6). With basolateral AE1 protein abundance being decreased in all three segments upon feeding (and with the most pronounced decrease in the proximal tubule; Fehsenfeld and Wood 2018), the effect observed with the application of the inhibitor DIDS basolaterally might mostly be due to targeting NBC1. Blocking NBC1-promoted reabsorption of HCO_3^- into the extracellular fluid would result in an increase of extracellular H^+ and therefore diminish the H^+ gradient and the H^+ back-flux as observed here. This finding emphasizes the importance of renal reabsorption of HCO_3^- for acid-base balance during metabolic acidosis especially in the proximal tubule.

V-H⁺-ATPase

Apical V-H^+-ATPase (HAT) is generally believed to promote H^+-secretion in branchial acid-secreting cells like peanut lectin agglutinin mitochondria rich cells (PNA^- MR) of the trout gill epithelium and in proton pump rich (HR) cells of zebrafish gills (Gilmour and Perry, 2009). In contrast, branchial base-secreting cells seem to possess a basolateral HAT as proposed for trout PNA^+ MR cells (Gilmour and Perry, 2009) and the branchial epithelium of stingrays (Piermarini and Evans, 2001). A similar distinction of cells can be made in the vertebrate kidney, with apical HAT in A-type intercalated cells (PNA^-; co-expressed with basolateral anion exchanger AE1) of the distal tubule, connecting segment and the collecting duct of the kidney cortex functioning as acid-secreting cells, whereas HAT is more ubiquitously expressed in B-type intercalated cells (PNA^+; co-expressed with apical pendrin) and is often localized in the basolateral membrane (Brown and Breton, 2000; Brown et al., 2009). In goldfish tubules, HAT appeared to localize

exclusively to the basolateral membrane of all three investigated segments of this study (Fehsenfeld and Wood, 2018). A basolateral HAT could indeed be important for the alkalinisation of the urine under control condition (Lawrence et al., 2015).

The pharmaceutical bafilomycin decreased H^+ flux in the proximal (Fig. 4) and distal tubule (Fig. 5), confirming a role for HAT in acid-base regulation of these tubule regions. With a basolateral HAT presumably pumping H^+ into the plasma, inhibiting this pathway would accumulate intracellular protons and result in a shift of the equilibrium for the intracellular carbonate system. Consequently, the generation of intracellular CO_2 would increase while diminishing both intracellular H^+ and HCO_3^-. The observed decrease in net H^+ flux upon blocking HAT could then be explained by the general decrease of intracellular protons available for basolateral, and possibly apical, transport, while also less HCO_3^- could be reabsorbed basolaterally via Na^+/HCO_3^- -cotransporter.

Carbonic anhydrase

Carbonic anhydrase is crucial for acid-base balance in virtually all systems (Gilmour and Perry, 2009). In addition to the predominant cytosolic isoform of the enzyme (CAII-like/ CAc) (Esbaugh et al., 2005; Gilmour and Perry, 2009), the kidney of freshwater teleosts expresses at least one membrane-bound carbonic anhydrase (CAIV) (Georgalis et al., 2006). CAIV is located apically and available to the tubular lumen in both mammals (Hamm et al. 2013; Schwartz et al. 2000) and fishes (Perry et al. 2003b; Georgalis et al. 2006), where it is proposed to help titrate filtered HCO_3^- with secreted H^+, thereby effecting HCO_3^- reabsorption from the urine. Intracellularly, carbonic anhydrase converts intracellular CO_2 into HCO_3^- and H^+ to then be returned to the extracellular fluid or secreted into the urine, respectively.

Blocking carbonic anhydrase in the present study decreased H^+ flux by 60% in all three investigated segments, indicating that the conversion of CO_2 contributes considerably to the secretion and/or reabsorption of acid-base equivalents, respectively. The inhibitor acetazolamide, however, is membrane-permeable and does not distinguish between different isoforms of the enzyme. Consequently, the present results do confirm that carbonic anhydrase is critical for acid secretion and/or base reabsorption in all three parts of the goldfish tubule, but do not reveal the site of action.

Acknowledgements

We thank Ryan Belowitz for help with the fish maintenance. Financial support was provided by Discovery Grants from the Natural Sciences and Engineering Research Council of Canada (NSERC) to MJO (NSERC PIN-2015-14139) and CMW (NSERC PIN-2017-03843). The authors would like to thank Dr. Scott P. Kelly (York University, Toronto) for donation of 2,4,6-triaminopyrimidine.

Competing Interests

The authors declare no competing interests.

Author Contributions

SF, DK, CMW, and MJO conceived the study; SF, DK, and MJO performed the experiments and analysed the data; SF wrote the first draft of the paper; all authors revised and approved of the final draft of the manuscript.

List of Abbreviations

A-IC / B-IC	A / B intercalated cells
AE	anion exchanger (Cl^-/HCO_3^-)
AMM	Ammoniagenesis
ASET2	Automated Scanning Electrode Technique version 2 software (Science Wares)
x_i	Buffering capacity (SIET)
CA	Carbonic anhydrase
C_B	background ion concentration in µmol L^{-1} (SIET)
CT	Connecting tubule
ΔC	Concentration gradient in mol cm^{-3} (SIET)
ΔV	Voltage gradient obtained from the software ASET2 in µV (SIET)
Δx	Distance between the two measuring points of electrode in cm (SIET)
D	Diffusion coefficient in cm^2 s^{-1} (SIET)
DIDS	4,4'-diisothiocyanatostilbene-2,2'-disulfonate
DT	Distal tubule
ECF	Extracellular fluid
EIPA	5-(N-ethyl-N-isopropyl)amiloride
HAT	$V\text{-}H^+$-ATPase
HR	Proton pump (HAT) rich cell
J	Flux in mol cm^{-2} s^{-1}
Ka	Acid dissociation constant (SIET)
NBC	Na^+/HCO_3^- cotransporter
NHE	Na^+/H^+ exchanger

$PNA^{+/-}$	Peanut lectin agglutinin cell
PT	Proximal tubule
S	slope of the SIET-electrode
SIET	Scanning Ion-selective Electrode Technique
TAP	2,4,6-triaminopyrimidine
TJ	Tight junction

References

Ambühl, P. M., Amemiya, M., Danczkay, M., Lötscher, M., Kaissling, B., Moe, O. W., Preisig, P. A. and Alpern, R. J. (1996). Chronic metabolic acidosis increases NHE3 protein abundance in rat kidney. *AJP Ren. Physiol.* 271, F917–F925.

Bayaa, M., Vulesevic, B., Esbaugh, A., Braun, M., Ekker, M. E., Grosell, M. and Perry, S. F. (2009). The involvement of SLC26 anion transporters in chloride uptake in zebrafish (*Danio rerio*) larvae. *J. Exp. Biol.* 212, 3283–3295.

Bobulescu, A., Di Sole, F. and Moe, O. W. (2005). Na^+/H^+ exchangers: physiology and link to hypertension and organ ischemia. *Curr. Opin. Nephrol. Hypertens.* 14(5), 485–494.

Brown, D. and Breton, S. (2000). H^+V-ATPase-dependent luminal acidification in the kidney collecting duct and the epididymis/vas deferens: vesicle recycling and transcytotic pathways. *J. Exp. Biol.* 203, 137–145.

Brown, D., Paunescu, T. G., Breton, S. and Marshansky, V. (2009). Regulation of the V-ATPase in kidney epithelial cells: dual role in acid–base homeostasis and vesicle trafficking. *J. Exp. Biol.* 212, 1762–1772.

Bucking, C., Landman, M. J. and Wood, C. M. (2010). The role of the kidney in compensating the alkaline tide, electrolyte load, and fluid balance disturbance associated with feeding in the freshwater rainbow trout, *Oncorhynchus mykiss*. *Comp. Biochem. Physiol. Part A.* 156, 74–83.

Chaillet, J. R. and Lopes, A. G. (1985). Basolateral Na-H exchange in the rabbit cortical collecting tubule. *J. Gen. Physiol.* 86, 798–812.

Chasiotis, H. and Kelly, S. P. (2008). Occludin immunolocalization and protein expression in goldfish. *J. Exp. Biol.* 211, 1524–1534.

Chasiotis, H. and Kelly, S. P. (2009). Occludin and hydromineral balance in *Xenopus laevis*. *J.*

Exp. Biol. 212, 287–296.

Curtis, B. J. and Wood, C. M. (1992). Kidney and urinary bladder responses of freshwater rainbow trout to isosmotic NaCl and $NaHCO_3$ infusion. *J. Exp. Biol.* 173, 181–203.

D'Silva, N. M., Donini, A. and O'Donnell, M. J. (2017). The roles of V-type H^+-ATPase and Na^+/K^+-ATPase in energizing K^+ and H^+ transport in larval *Drosophila* gut epithelia. *J. Insect Physiol.* Elsevier Ltd, 98, 284–290.

Dantzler, W. H. (2016) *Comparative physiology of the vertebrate kidney*. 2nd ed. New York: Springer Science+Business Media LLC.

Donini, A. and O'Donnell, M. J. (2005). Analysis of Na^+, Cl^-, K^+, H^+ and NH_4^+ concentration gradients adjacent to the surface of anal papillae of the mosquito *Aedes aegypti*: application of self-referencing ion-selective microelectrodes. *J. Exp. Biol.* 208, 603–610.

Esbaugh, A. J., Perry, S. F., Bayaa, M., Georgalis, T., Nickerson, J., Tufts, B. L. and Gilmour, K. M. (2005). Cytoplasmic carbonic anhydrase isozymes in rainbow trout *Oncorhynchus mykiss*: comparative physiology and molecular evolution. *J. Exp. Biol.* 208, 1951–1961.

Fehsenfeld, S. and Weihrauch, D. (2016). Mechanisms of acid–base regulation in seawater-acclimated green crabs (*Carcinus maenas*). *Can. J. Zool.* 94, 95–107.

Fehsenfeld, S. and Wood, C. M. (2018). Section-specific expression of acid-base and ammonia transporters in the kidney tubules of the goldfish *Carassius auratus* and their responses to feeding. *AJP Ren. Physiol.* 315, F1565–F1582.

Georgalis, T., Gilmour, K. M., Yorston, J. and Perry, S. F. (2006). Roles of cytosolic and membrane-bound carbonic anhydrase in renal control of acid-base balance in rainbow trout, *Oncorhynchus mykiss*. *AJP Ren. Physiol.* 291, F407–F421.

Gilmour, K. M. and Perry, S. F. (2009). Carbonic anhydrase and acid-base regulation in fish. *J.*

Exp. Biol. 212, 1647–1661.

Hamm, L. L., Alpern, R. J. and Preisig, P. A. (2013). Cellular mechanisms of renal tubular acidification. in Alpern, R. J., Moe, O. W., and Caplan, M. (eds.) *Seldin and Giebisch's The Kidney*. 5th ed. Elsevier Inc., pp. 1917–1978.

Hamm, L. L., Nakhoul, N. and Hering-Smith, K. S. (2015). Acid-base homeostasis. *Clin. J. Am. Soc. Nephrol.* 10, 2232–2242.

Hammer, Ø., Harper, D. A. T. and Ryan, P. D. (2001). PAST: Paleontological statistics software package for education and data analysis. *Palaeontol. Electron.* 4(1), 1–9.

Handlogten, M. E., Osis, G., Lee, H.-W., Romero, M. F., Verlander, J. W. and Weiner, I. D. (2015). NBCe1 expression is required for normal renal ammonia metabolism. *AJP Ren. Physiol.* 309, 658–666.

Hoar, W. S. and Hickman, C. P. (1975) *A laboratory companion for general and comparative physiology*. 2nd ed. Prentice Hall.

Hou, J., Rajagopal, M. and Yu, A. S. L. (2013). Claudins and the kidney. *Annu. Rev. Physiol.* 75, 479–501.

Van Itallie, C. M., Holmes, J., Bridges, A., Gookin, J. L., Coccaro, M. R., Proctor, W., Colegio, O. R. and Anderson, J. M. (2008). The density of small tight junction pores varies among cell types and is increased by expression of claudin-2. *J. Cell Sci.* 121, 298–305.

Ivanis, G., Braun, M. and Perry, S. F. (2008). Renal expression and localization of SLC9A3 sodium/hydrogen exchanger and its possible role in acid-base regulation in freshwater rainbow trout (*Oncorhynchus mykiss*). *AJP Regul. Integr. Comp. Physiol.* 295, R971–R978.

Kolosov, D., Bui, P., Chasiotis, H. and Kelly, S. P. (2013). Claudins in teleost fishes. *Tissue Barriers*, 1(3), e25391.

Kolosov, D., Bui, P., Donini, A., Wilkie, M. P. and Kelly, S. P. (2017). A role for tight junction-associated MARVEL proteins in larval sea lamprey (*Petromyzon marinus*) osmoregulation. *J. Exp. Biol.* 220, 3657–3670.

Kolosov, D., Chasiotis, H. and Kelly, S. P. (2014). Tight junction protein gene expression patterns and changes in transcript abundance during development of model fish gill epithelia. *J. Exp. Biol.* 217, 1667–1681.

Kolosov, D. and Kelly, S. P. (2013). A role for tricellulin in the regulation of gill epithelium permeability. *AJP Regul. Integr. Comp. Physiol.* 304, R1139–R1148.

Kolosov, D. and Kelly, S. P. (2018). Tricellular tight junction-associated angulins in the gill epithelium of rainbow trout. *AJP Regul. Integr. Comp. Physiol.* 315, R312–R322.

Lawrence, M. J., Wright, P. A. and Wood, C. M. (2015). Physiological and molecular responses of the goldfish (*Carassius auratus*) kidney to metabolic acidosis, and potential mechanisms of renal ammonia transport. *J. Exp. Biol.* 218, 2124–2135.

McDonald, D. G. and Wood, C. M. (1981). Branchial and renal acid and ion fluxes in the rainbow trout, *Salmo gairdneri*, at low environmental pH. *J. Exp. Biol.* 93, 101–118.

McKinney, T. D. and Burg, M. B. (1977). Bicarbonate transport by rabbit cortical collecting tubules - Effect of acid and alkali loads in vivo on transport in vitro. *J. Clin. Invest.* 60, 766–768.

Messerli, M. A., Robinson, K. R. and Smith, P. J. S. (2006). Electrochemical sensor applications to the study of molecular physiology and analyte flux in plants. in Volkov, A. G. (ed.) *Plant Physiology: Theory and Methods*. Berlin Heidelberg: Springer Berlin Heidelberg, pp. 73–107.

O'Neil, R. and Hayhurst, R. A. (1985). Functional differentiation of cell types of cortical collecting duct. *AJP Ren. Physiol.* 248, F449–F453.

Pacey, E. K. and O'Donnell, M. J. (2014). Transport of H^+, Na^+ and K^+ across the posterior

midgut of blood-fed mosquitoes (*Aedes aegypti*). *J. Insect Physiol*. Elsevier Ltd, 61, 42–50.

Perry, S. F. and Fryer, J. N. (1997). Proton pumps in the fish gill and kidney. *Fish Physiol. Biochem.* 17, 363–369.

Perry, S. F., Furimsky, M., Bayaa, M., Georgalis, T., Shahsavarani, A., Nickerson, J. G. and Moon, T. W. (2003a). Integrated responses of Na^+/ HCO_3^- cotransporters and V-type H^+-ATPases in the fish gill and kidney during respiratory acidosis. *Biochim. Biophys. Acta.* 1618, 175–184.

Perry, S. F. and Gilmour, K. M. (2006). Acid-base balance and CO_2 excretion in fish: Unanswered questions and emerging models. *Respir. Physiol. Neurobiol.* 154, 199–215.

Perry, S. F., Shahsavarani, A., Georgalis, T., Bayaa, M., Furimsky, M. and Thomas, S. L. Y. (2003b). Channels, pumps, and exchangers in the gill and kidney of freshwater fishes: their role in ionic and acid-base regulation. *J. Exp. Zool.* 300A, 53–62.

Piermarini, P. M. and Evans, D. H. (2001). Immunochemical analysis of the vacuolar proton-ATPase B-subunit in the gills of a euryhaline stingray (*Dasyatis sabina*): effects of salinity and relation to Na^+/K^+-ATPase. *J. Exp. Biol.* 204, 3251–3259.

Pineros, M. A., Shaff, J. E. and Kochian, L. V (1998). Development, characterization, and application of a cadmium-selective microelectrode for the measurement of cadmium fluxes in roots of *Thlaspi* species and wheat. *Plant Physiol.* 116, 1393–1401.

Reilly, B. D., Cramp, R. L., Wilson, J. M., Campbell, H. A. and Franklin, C. E. (2011). Branchial osmoregulation in the euryhaline bull shark, *Carcharhinus leucas*: a molecular analysis of ion transporters. *J. Exp. Biol.* 214, 2883–2895.

Ridderstrale, Y., Kashgarian, M., Koeppen, B., Giebisch, G., Stetson, D., Ardito, T. and Stanton, B. (1988). Morphological heterogeneity of the rabbit collecting duct. *Kidney Int.* 34(5), 655–670.

Riggs, A. F. (1988). The Bohr effect. *Annu. Rev. Physiol.* 50, 181–204.

Roa, J. N., Munévar, C. L. and Tresguerres, M. (2014). Feeding induces translocation of vacuolar proton ATPase and pendrin to the membrane of leopard shark (*Triakis semifasciata*) mitochondrion-rich gill cells. *Comp. Biochem. Physiol. Part A.* 174, 29–37.

Sakai, T. (1985). The structure of the kidney from the freshwater teleost *Carassius auratus*. *Anat. Embryol. (Berl).* 171, 31–39.

Schwartz, G. J., Kittelberger, A. M., Barnhart, D. A. and Vijayakumar, S. (2000). Carbonic anhydrase IV is expressed in H^+-secreting cells of rabbit kidney. *AJP Ren. Physiol.* 278, F894–F904.

Seshadri, R. M., Klein, J. D., Smith, T., Sands, J. M., Handlogten, M. E., Verlander, J. W. and Weiner, I. D. (2006). Changes in subcellular distribution of the ammonia transporter, Rhcg, in response to chronic metabolic acidosis. *AJP Ren. Physiol.* 290, F1443-1452.

Simon, E., Martin, D. and Buerkert, J. (1985). Contribution of individual superficial nephron segments to ammonium handling in chronic metabolic acidosis in the rat. *J. Clin. Invest.* 76, 855–864.

Skelton, L. A., Boron, W. F. and Zhou, Y. (2010). Acid-base transport by the renal proximal tubule. *J. Nephrol.* 23(0 16), S4-18.

Smith, P. J. S., Sanger, R. H. and Jaffe, L. F. (1994). The vibrating Ca^{2+} electrode: a new technique for detecting plasma membrane regions of Ca^{2+} influx and efflux. *Methods Cell Biol.* 40, 115–134.

Soleimani, M., Greeley, T., Petrovic, S., Amlal, H., Kopp, P., Burnham, C. E., Greeley, T., Wang, Z., Amlal, H., Kopp, P. and Burnham, C. E. (2001). Pendrin: an apical $Cl^-/OH^-/HCO_3^-$ exchanger in the kidney cortex. *AJP Ren. Physiol.* 280, F356–F364.

Somero, G. N. (1986). Protons, osmolytes, and fitness of internal milieu for protein function. *Am. J. Physiol. - Regul. Integr. Comp. Physiol.* 251(2), R197–R213.

Sussman, C. R., Zhao, J., Plata, C., Lu, J., Daly, C., Angle, N., Dipiero, J., Drummond, I. A., Teranishi, K., Mekuchi, M. and Kaneko, T. (2013). Expression of sodium/hydrogen exchanger 3 and cation-chloride cotransporters in the kidney of Japanese eel acclimated to a wide range of salinities. *Comp. Biochem. Physiol. Part A.* 164, 333–343.

Tresguerres, M., Katoh, F., Fenton, H., Jasinska, E. and Goss, G. G. (2005). Regulation of branchial V-H^+-ATPase, Na^+/K^+-ATPase and NHE2 in response to acid and base infusions in the Pacific spiny dogfish (*Squalus acanthias*). *J. Exp. Biol.* 208, 345–354.

Tresguerres, M., Parks, S. K., Wood, C. M. and Goss, G. G. (2007). V-H^+-ATPase translocation during blood alkalosis in dogfish gills: interaction with carbonic anhydrase and involvement in the postfeeding alkaline tide. *Am. J. Physiol. - Regul. Integr. Comp. Physiol.* 292, R2012–R2019.

Wang, X. and Kurtz, I. (1990). H^+/base transport in principal cells characterized by confocal fluorescence imaging. *American Journal of Physiology - Cell Physiology*, 259, C365–C373.

Weiner, D. and Hamm, L. L. (1990). Regulation of intracellular pH in the rabbit cortical collecting tubule. *J. Clin. Invest.* 85, 274–281.

Weiner, I. D. and Verlander, J. W. (2013). Renal ammonia metabolism and transport. *Compr. Physiol.* 3(1), 201–220.

Weiner, I. D. and Verlander, J. W. (2017). Ammonia transporters and their role in acid-base balance. *Physiol. Rev.* 97, 465–494.

Wheatly, M. G., Hobe, H. and Wood, C. M. (1984). The mechanisms of acid-base and ionoregulation in the freshwater rainbow trout during environmental hyperoxia and subsequent normoxia. II. The role of the kidney. *Respir. Physiol.* 55, 155–173.

Wood, C. M. (1988). Acid-base and ionic exchanges at gills and kidney after exhaustive exercise in the rainbow trout. *J. Exp. Biol.* 136, 461–481.

Wood, C. M., Bucking, C. and Grosell, M. (2010). Acid-base responses to feeding and intestinal Cl^- uptake in freshwater- and seawater-acclimated killifish, *Fundulus heteroclitus*, an agastric euryhaline teleost. *J. Exp. Biol.* 213, 2681–2692.

Wood, C. M., Milligan, C. L. and Walsh, P. J. (1999). Renal responses of trout to chronic respiratory and metabolic acidoses and metabolic alkalosis. *AJP Regul. Integr. Comp. Physiol.* 277, R482–R492.

Wright, P. A., Wood, C. M. and Wilson, J. M. (2014). Rh versus pH: the role of Rhesus glycoproteins in renal ammonia excretion during metabolic acidosis in a freshwater teleost fish. *J. Exp. Biol.* 217, 2855–2865.

Figures

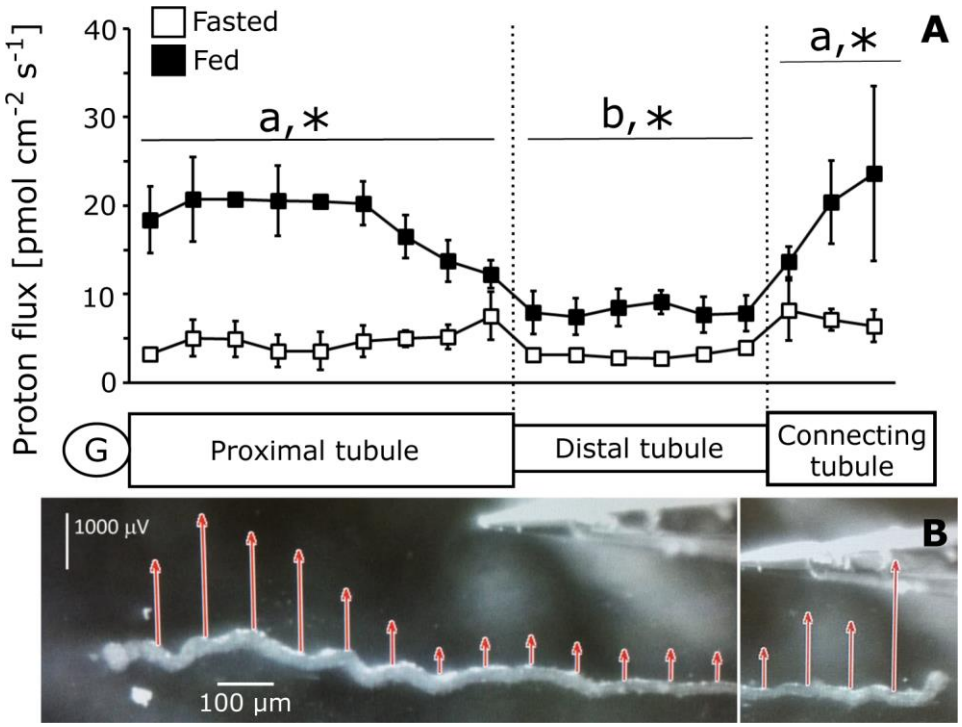

Figure 1. Proton fluxes along the nephron of fasted and fed goldfish *Carassius auratus*. (A) Scanning ion micro-electrode measurements of H^+ fluxes in renal proximal, distal and connecting tubules in fasted (open squares) and fed (black squares) goldfish. Lower case letters indicate significant differences among mean fluxes for each tubules segment in fed animals, while asterisks denote significant differences in the mean flux in the respective tubule segment between fed and fasted animals (two-way ANOVA and Tukey's post-hoc analysis with $p < 0.05$). Data are represented as means ± SE (N = 5). (B) Representative visualisation of calculated H^+ flux in the nephron of a fed goldfish as depicted by ASET2 software (arrow length indicates magnitude, arrowheads direction of the flux). H^+ flux was directed from the tubule lumen towards the external medium. Due to the length of the tissue, the figure was generated by

combining two screenshots. Both screenshots have been overlaid as much as possible and the right image was then cropped to match the transition from the left (indicated by white space between both screenshots).

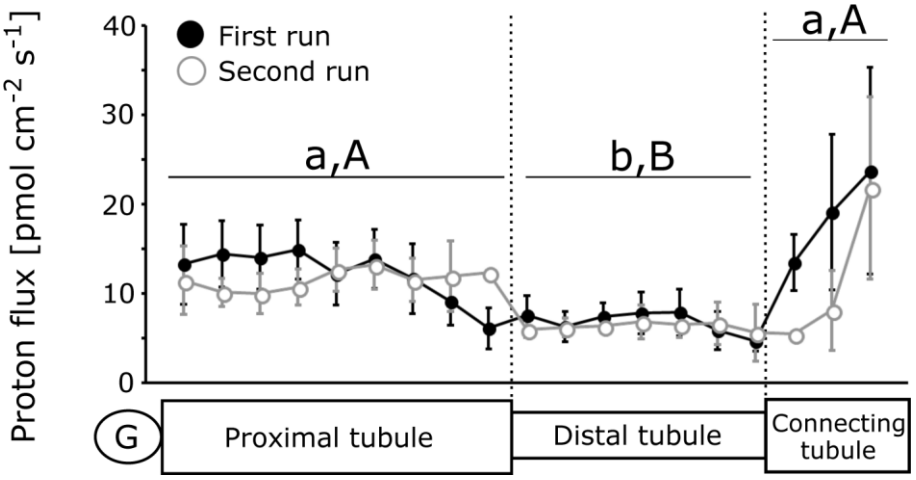

Figure 2. Effect of time on H^+ flux along the renal tubules of fed goldfish. Re-scanning of the same tubule to exclude changes in tissue viability for inhibitor experiments. After a first scan in 100 μm increments, Ringer solution was exchanged and left for 10 min before a second scan of the same tubule was performed. Letters indicate significant differences among mean fluxes for each tubule segment in fed animals (lower case, first run; upper case, second run); no difference was found between the first and second run (repeated measures two-way ANOVA with Tukey's post-hoc analysis, N = 3). Data are represented as means ± SE.

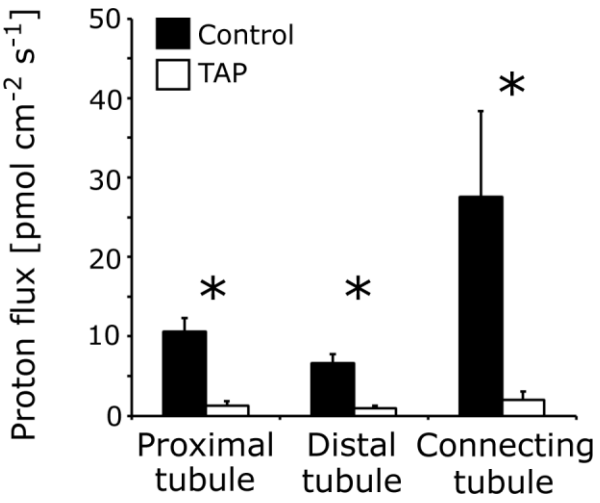

Figure 3. Effects on renal tubule H^+ back-flux in preparations from fed goldfish by inhibition of the paracellular pathway. Data are represented as means ± SE. Asterisks denote significant differences between H^+ flux with control saline (black bars) and the application of 10 mmol L^{-1} 2,4,6-triaminopyrimidine (TAP; white bars; Student's paired t-test with $p < 0.05$ and $N = 4$).

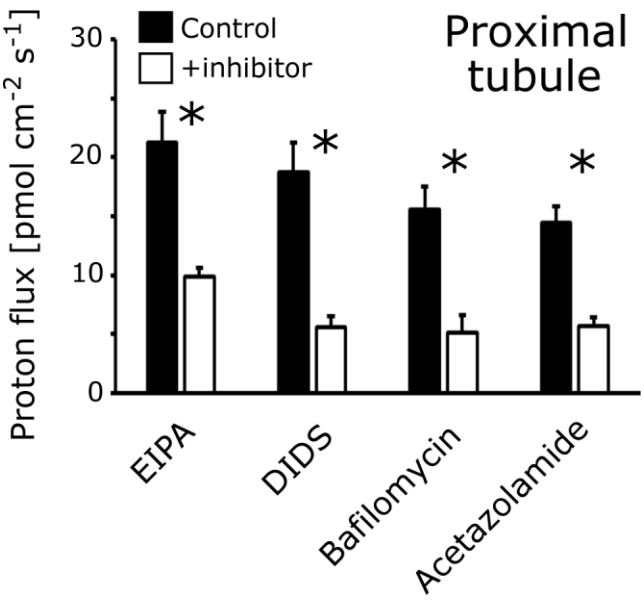

Figure 4. Effects on H^+ back-flux of inhibitors for acid-base relevant epithelial transporters in the proximal tubule in preparations from fed goldfish. H^+-flux was directed from the lumen into the extracellular fluid and decreased with the application of all inhibitors. 100 μmol L^{-1} EIPA (5-(N-ethyl-N-isopropyl)amiloride) for Na^+/H^+-exchangers; 100 μmol L^{-1} DIDS (4,4'-diisothiocyanatostilbene-2,2'-disulfonate) for HCO_3^--transporters; 5 μmol L^{-1} bafilomycin for V-H^+-ATPase, 1 μmol L^{-1} acetazolamide for carbonic anhydrase. Asterisks denote significant differences between H^+ back-flux with control saline (black bars) and the application of the respective inhibitor (white bars) for the respective transporters (Student's paired t-test with $p < 0.05$ and $N = 6$-8). Data are represented as means ± SE.

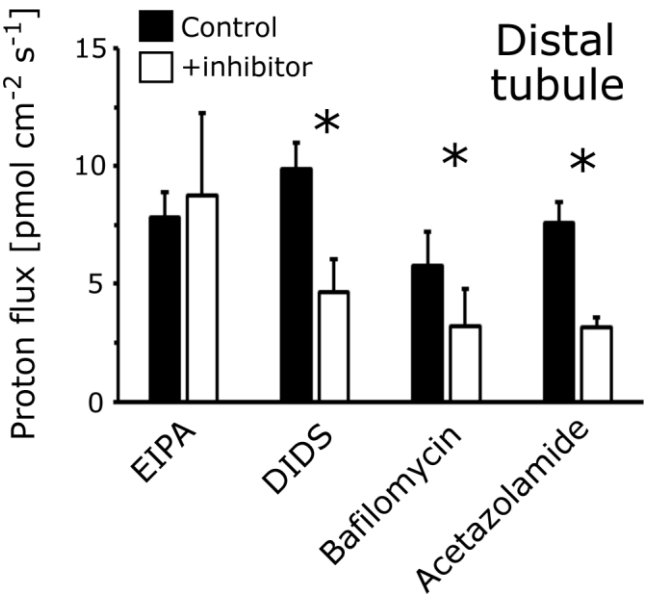

Figure 5. Effects on H^+ back-flux of inhibitors for acid-base relevant epithelial transporters in the distal tubule in preparations from fed goldfish. H^+-flux was directed from the lumen into the extracellular fluid and decreased with the application of most inhibitors. 100 μmol L^{-1} EIPA (5-(N-ethyl-N-isopropyl)amiloride) for Na^+/H^+-exchangers; 100 μmol L^{-1} DIDS (4,4'-diisothiocyanatostilbene-2,2'-disulfonate) for HCO_3^--transporters; 5 μmol L^{-1} bafilomycin for V-H^+-ATPase, 1 μmol L^{-1} acetazolamide for carbonic anhydrase. Asterisks denote significant differences between H^+ back-flux with control saline (black bars) and the application of the respective inhibitor (white bars) for the respective transporters (Student's paired t-test with $p < 0.05$ and N = 6-8). Data are represented as means ± SE.

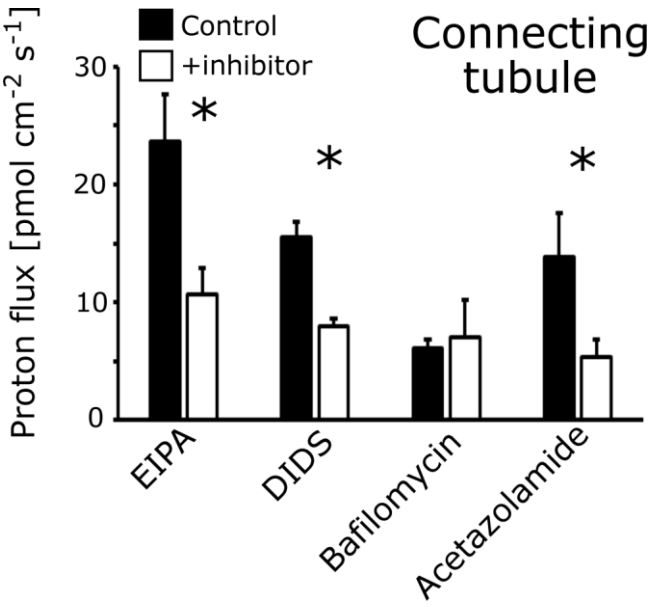

Figure 6. Effects on H^+ back-flux of inhibitors for acid-base relevant epithelial transporters in the connecting tubule in preparations from fed goldfish. H^+-flux was directed from the lumen into the extracellular fluid and decreased with the application of most inhibitors. 100 μmol L^{-1} EIPA (5-(N-ethyl-N-isopropyl)amiloride) for Na^+/H^+-exchangers; 100 μmol L^{-1} DIDS (4,4'-diisothiocyanatostilbene-2,2'-disulfonate) for HCO_3^--transporters; 5 μmol L^{-1} bafilomycin for V-H^+-ATPase, 1 μmol L^{-1} acetazolamide for carbonic anhydrase. Asterisks denote significant differences between H^+-back flux with control saline (black bars) and the application of the respective inhibitor (white bars) for the respective transporters (Student's paired t-test with $p < 0.05$ and N = 6-8). Data are represented as means ± SE.

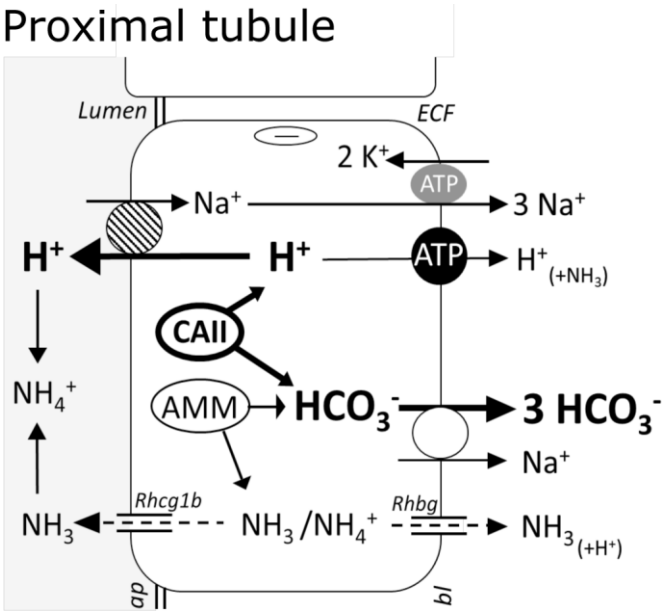

Figure 7. Proposed model for the renal fluxes of H^+ and other acid-base equivalents in the proximal tubule of the goldfish, *Carassius auratus*. Solid lines represent primary and secondary active ion transport, dashed lines are indicative of channels that allow for bi-directional flow, and wavy lines represent vesicular transport. The negative electric potential of the cell towards both the plasma/extracellular fluid as well as the urine/lumen is indicated by the oval containing a minus. Major contributors to acid-base regulation are indicated in bold lines and text. We propose the proximal tubule to mainly contribute to HCO_3^- reabsorption into the extracellular fluid, as well as H^+ secretion into the luminal space, comparable to what has been observed in the mammalian kidney. H^+ is suggested to mainly be generated by cytoplasmic carbonic anhydrase (CAII-like) and secreted by apical Na^+/H^+-exchanger (NHE3). Apical Rhesus proteins (Rhcg1b/Rhcg2) potentially titrate urine H^+ and trap it in the form of NH_4^+ in the lumen. Apical Na^+ entry via NHE3 is energized by the basolateral Na^+/K^+-ATPase. H^+ is also partly reabsorbed into the plasma via basolateral V-H^+-ATPase (in contrast to apical V-H^+-

ATPase in mammals) and might help to titrate plasma NH_3 reabsorbed via Rhesus protein Rhbg to "trap" NH_4^+. The major source for HCO_3^- in this tubule region likely is ammoniagenesis (AMM) as observed in mammals. HCO_3^- is reabsorbed into the extracellular fluid via Na^+/HCO_3^- cotransport (likely electrogenic 1:3 by NBC1). The processes depicted here indicate a proximal tubule cell in goldfish to resemble an intermediate between mammalian proximal tubule cells and B-intercalated cells of the collecting duct.

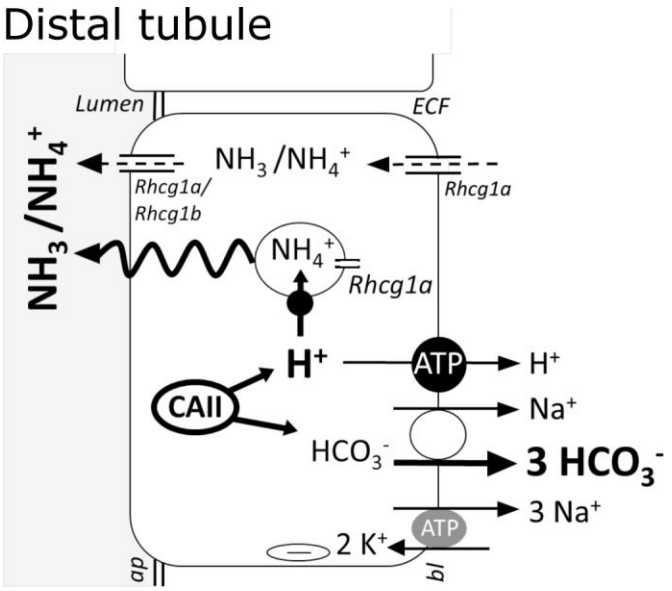

Figure 8. Proposed model for the renal fluxes of H^+ and other acid-base equivalents in the distal tubule of the goldfish, *Carassius auratus*. Please see Fig. 7 caption for formatting details and sources. The distal tubule may contribute substantially to NH_3/NH_4^+ secretion into the luminal space, as well as HCO_3^- reabsorption into the extracellular fluid. In contrast to mammals it may play only a minor role in direct H^+-secretion into the lumen. As in the proximal tubules, cytoplasmic carbonic anhydrase (CAII-like) may play the major role in the generation of H^+. H^+ and HCO_3^- are reabsorbed basolaterally by V-H^+-ATPase and Na^+/HCO_3^- cotransport (likely electrogenic 1:3 by NBC1). NBC1-mediated reabsorption of HCO_3^- into the plasma would be driven by the negative membrane potential generated by basolateral Na^+/K^+-ATPase. NH_3/NH_4^+ secretion via apical Rhcg1a and/or 1b, and basolateral Rhcg1a may be supported by exocytosis of acidified vesicles as proposed for branchial epithelia in green crabs *Carcinus maenas* (Fehsenfeld and Weihrauch, 2016) and rats experiencing a metabolic acidosis (Seshadri et al., 2006).

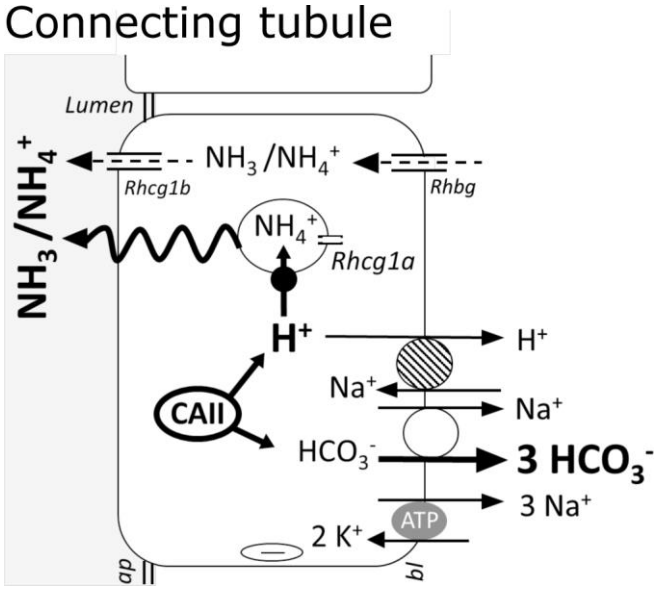

Figure 9. Proposed model for the renal fluxes of H^+ and other acid-base equivalents in the connecting tubule of the goldfish, *Carassius auratus*. Please see Fig. 7 caption for formatting details and sources. Like the distal tubule, the connecting tubule is proposed to contribute mostly to NH_3/NH_4^+ secretion into the luminal space, as well as HCO_3^- reabsorption into the extracellular fluid. In contrast to the distal tubule, however, (i) basolateral exit of H^+ into the extracellular fluid is likely rather promoted by basolateral Na^+/H^+-exchanger and not basolateral V-H^+-ATPase, and (ii) NH_3/NH_4^+ secretion might be accomplished rather via basolateral Rhesus protein Rhbg and apical Rhcg1b with less involvement of membrane-bound Rhcg1a. The presence of basolateral Na^+/H^+-exchanger and Na^+/HCO_3^- cotransporter (likely electrogenic 1:3 NBC1) suggests the connecting tubule to be composed of cells comparable to mammalian principal cells of the connecting segment/collecting duct of the kidney.